Dynamics on Microcomposite Catalytic Surfacces: The Effect of Active Boundaries

Stanislav Y. Shvartsman,[1] Eckart Shütz,[2] Ronald Imbihl,[2] and Ioannis G. Kevrekidis[1,*]

[1]*Department of Chemical Engineering, Princeton University, Princeton, New Jersey 08544*

[2]*Department of Physical Chemistry and Electrochemistry, Universitaet Hannover, Callinstrasse 3-3a, D-30167 Hannover, Germany*

(Received 7 May 1999)

We report experimental and theoretical studies of reaction dynamics on Pt/Rh and Pt/TiO_2 microcomposite catalytic surfaces. Both steady and dynamic behaviors are dominated by reaction fronts initiated at the interface between different catalytic components. Our analysis links the bifurcation behavior of reactive composites with active boundaries to this transient phenomenon of front initiation.

PACS numbers: 82.40.Ck, 05.45.Jn, 82.40.Bj, 82.65.Jv

The presence of controlled heterogeneities in a reactive medium introduces a new dimension to the complexity of dynamic pattern formation. The shape and length scales of the medium heterogeneity become nontrivially linked to the intrinsic length and time scales of reaction and transport in each active component. While the resulting dynamic phenomenology becomes quickly too rich to classify, understanding certain well-defined limiting regimes can be useful in providing guidelines for the design of composite reactive materials with nonlinear properties.

In this Letter we address, through a combination of experiments and modeling, a class of structured nonlinear materials: two-dimensional microcomposite catalysts. Our goal is twofold: in addition to investigating dynamics in *structured* bistable media [1], we take steps towards understanding reactive properties of catalytic materials with several active components interdispersed at a scale representative of patterns spontaneously forming in these systems [2].

Consider a catalytic medium (a Pt single crystal surface) on which a chemical reaction (NO reduction) occurs. Instabilities due to kinetic nonlinearities are known to lead to steady state multiplicity. We study the effect on these dynamics of *active inhomogeneities*: patches with different kinetic/transport properties dispersed in, and diffusively coupled to, the original catalyst matrix. A systematic experimental study of inclusion size effects, coupled with mechanistic and phenomenological modeling, lays the foundation for a comprehensive picture of the dynamic and bifurcation behavior of the microdesigned medium. In particular, we study composite ignition and explore its bifurcation dependence on component geometry (specifically, inclusion size). Dynamic imaging [with photoelectron emission microscopy, (PEEM)] of NO reduction on microdesigned Pt/Rh and Pt/TiO_2 catalysts shows that reaction fronts originating at the matrix/inclusion interface constitute key events in overall composite surface behavior. Bistability ("kinetic hysteresis") of both the matrix and the inclusions of the composite surface lies at the heart of the observed phenomenology. Inspection of the "backbone" of the surface reaction mechanism,

$$
\begin{aligned}
NO_{ads} + * &\rightarrow N_{ads} + O_{ads} && (R_1),\\
2N_{ads} &\rightarrow N_2 + 2* && (R_2),\\
2H_{ads} + O_{ads} &\rightarrow H_2O + 3* && (R_3),\\
CO_{ads} + O_{ads} &\rightarrow CO_2 + 2* && (R_4),
\end{aligned}
$$

reveals that empty sites (*), necessary for the initiation of the rate limiting step (R_1), are regenerated in excess by the subsequent steps R_{2-4}. Bistability results from the balance between this autocatalytic generation of empty sites and their removal due to chemisorption. At fixed external conditions the surface can exist in two states differing in the overall amount of empty sites. Large differences of adsorbate coverages (especially O_{ads}) between these states give rise to a sharp contrast in PEEM, used here to visualize the spatiotemporal catalytic dynamics: the unreactive/reactive branches of the kinetic hysteresis appear dark/bright in the PEEM image of the surface.

Kinetic bistability coupled with diffusion is responsible for constant shape traveling concentration fronts on the surface; as we illustrate here, controlled heterogeneities can be designed to initiate such fronts. We design *controlled* heterogeneities through a multistep lithographic process leading to a surface on which areas of "bare" Pt(100) are surrounded by an $\approx$300 Å layer of either Rh or TiO_2 [3]. Figure 1 demonstrates that a step change in the operating conditions can lead to a spatially nonuniform transient phenomenon on the surface: here, a reaction front is generated at the boundary separating the catalytic components. Changing P_{H_2} from 2×10^{-6} to 7×10^{-6} mbar leads to the development of a bright rim at the Pt/Rh interface and initiates a front propagating *outwards* from the boundary. The front moving at velocities of $\sim 1 \mu$m/s leaves the Rh surface in the reactive (PEEM bright) state.

Our analysis of boundary initiated transitions starts by posing a reaction diffusion problem for a *model* Pt/Rh microcomposite: We envision a periodic array of alternating Pt/Rh stripes and focus on one-half of a unit cell of such a "crystal." Consistent mechanistic models for surface chemistry of NO reduction on surfaces of both metals [4], accounting for time evolution of coverages (θ) of six experimentally confirmed surface species (NO, N, O, H,

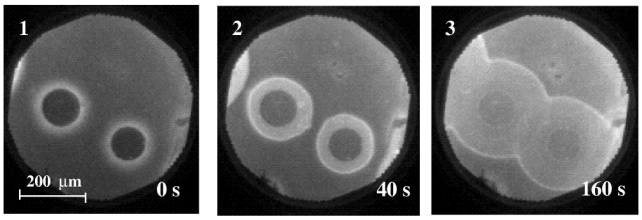

FIG. 1. PEEM images of the microstructured Pt(100)/Rh surface showing a transition from the unreactive, oxygen covered state to the reactive, largely oxygen-free state in the NO + H_2 reaction. Reaction fronts nucleate at the perimeter of the dark circles (frame 1)which represent circular Pt(100) domains surrounded by Rh. The transition was initiated by a step change in P_{H_2}; $P_{NO} = 2 \times 10^{-6}$ mbar, $T = 473$ K.

NH, and NH_3), robustly predict steady state multiplicity. The predicted bifurcation diagrams (in terms of θ_O as a function of P_{H_2}, at P_{NO}, and T corresponding to experimental conditions of Fig. 1) are shown in Fig. 2(a). As P_{H_2} is increased, each metal undergoes transition (through a saddle-node bifurcation) to a surface state with low θ_O (seen as a dark/bright transition in experiments). The transition is accompanied by an increase of θ_N and θ_H, and is manifested by the corresponding changes in steady reaction rates [see Fig. 2(b)]. The bifurcation is predicted to happen earlier (lower P_{H_2})for Pt; this correlates with higher/lower binding energies of H/O species for this metal. It is then conceivable that, for the appropriate range of P_{H_2}, "extinguished" Rh on a composite surface might lie next to "ignited" Pt.

In our reaction-diffusion model we require continuity of coverages and fluxes of each species at the Pt/Rh interface. Figures 2(c) and 2(d) shows simulation results of a boundary-initiated ignition event; T and P_{NO} are set to the values corresponding to the experiment in Fig. 1(c), and the same step in P_{H_2} is administered. This step change would bring a pure Pt surface to a unique, stable (PEEM-bright) steady state, while a pure Rh surface would remain on the unreactive branch of its bistable regime. We observe that the Pt component of the composite very quickly (within $\approx$1 s) undergoes transition to a state which, for all practical purposes, coincides with the pure-Pt reactive steady state at this P_{H_2}. Most of the Rh domain initially undergoes a transient to a state that practically coincides with the pure Rh unreactive steady state at this P_{H_2}. At the same time, concentration gradients in *all* surface species created at the material interface initiate a front that sweeps the Rh domain, bringing it to the low oxygen coverage, pure Rh reactive state; the predicted speed of such a developed front corresponds closely to the experimentally measured value of ~ 1 μm/s.

The 6 adspecies, 15 surface-reactions' model is only semiquantitative in nature; a more realistic account of catalytic dynamics on composites *must* address alloying between metals, the strongly non-Fickian character of surface diffusion, Pt surface reconstruction, as well as the presence of surface defects [5]. The chemistry and phenomenology of boundary-induced dynamic events, however, occurring due to species fluxes at the material interface, appear to be adequately captured. This analysis interprets the experiment in Fig. 1 as a boundary-induced, front-mediated transition between different branches of kinetic hysteresis.

A detailed bifurcation picture of the behavior associated with boundary-induced ignitions is developed using a phenomenological reaction-diffusion model. Consider half of the unit cell of a striped ("A/B") medium:

$$
\begin{aligned}
&x \in (0, L_A) : u_t^A = D u_{xx}^A + F(u^A, \alpha_A, \lambda)\,, \\
&x \in (L_A, L_B + L_A) : u_t^B = D u_{xx}^B + F(u^B, \alpha_B, \lambda)\,, \\
&u_x^B|_{L_B+L_A} = 0, \qquad u_x^A|_0 = 0\,, \\
&u_x^A|_{L_A} = u_x^B|_{L_A}\,, \qquad u^A|_{L_A} = u^B|_{L_A}\,.
\end{aligned}
$$

The cubic kinetic expression $u - u^3 + \alpha + \lambda$ models hysteresis in the dependence of the stationary solutions $u_s(\lambda)$ of $F(u_s, \lambda) = 0$ on λ (at constant α). Choosing $\alpha_A \neq \alpha_B$ ($\alpha_A = 0$, $\alpha_B = 1$) makes the boundaries of the hysteresis different for the "materials" A and B. We describe the composite system behavior using the term "ignited/extinguished," respectively, for states of the components that are practically identical to the corresponding ignited/extinguished steady state branches of the pure materials.

Figure 3(a) shows a *fragment* of the one-parameter bifurcation diagram of a 50/50 ($L_A = L_B$) A/B composite with respect to λ at a total length of 30. A wide range of bistability corresponds to the coexistence of "nonuniform" stable solutions with "uniform" ones: stable solutions where both components of the composite are at an ignited

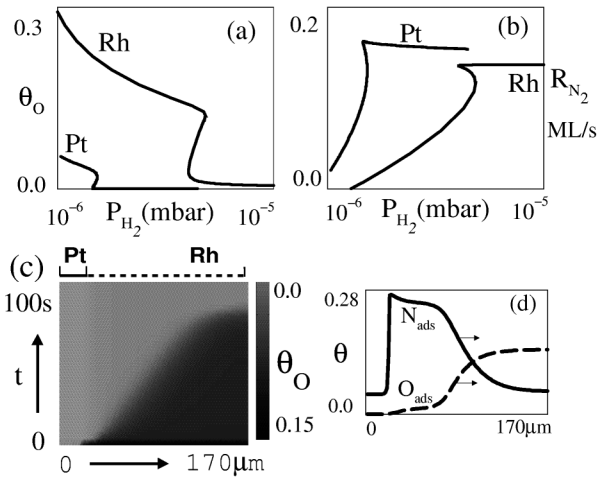

FIG. 2. (a),(b) NO/H_2 reaction model: Steady state multiplicity in terms of oxygen coverage (a) and rate of nitrogen production (b). (c) Spatiotemporal evolution of oxygen coverage on a Pt/Rh striped composite accompanying a step change in P_{H_2}. (d) Instantaneous profile of oxygen and nitrogen adspecies in a front developed across the composite.

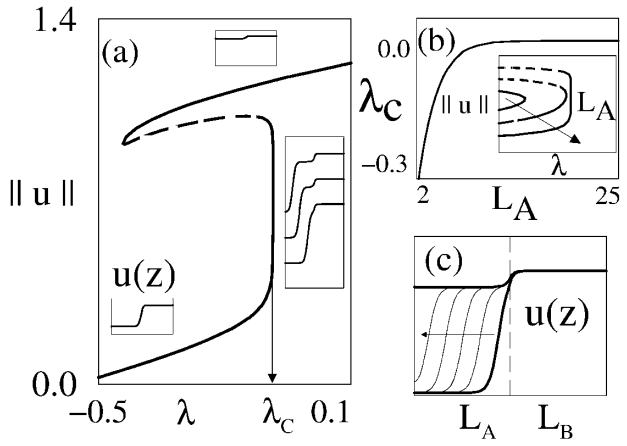

FIG. 3. (a) Steady state bifurcation diagram illustrating the transition from partially (lower inset) to fully (upper inset) ignited states of a bistable composite. Insets: steady state profiles, including a sequence of nonuniform frontlike states (middle inset). (b) Two-parameter continuation of the "partial to full ignition" turning points. (c) Transient from a partially to a fully ignited state mediated by front propagation.

state. The boundaries of the existence of such nonuniform solutions correspond to two instabilities [for clarity, only the right one, λ_c, is shown in Fig. 3(a)] mediating the transition to the uniform states. This instability at λ_c is associated with precisely the ignition events initiated at the boundary with an ignited component on which we focus here. Fixing the length of the ignited component (L_B), and analyzing the dependence of λ_c on L_A, we notice two simultaneous trends. As L_A is increased the value of λ at the ignition turning point (λ_c) approaches an asymptotic value; at the same time the part of the diagram in the neighborhood of the turning point becomes progressively flat [Fig. 3(b), inset]. At large L_A there is an apparently vertical part of the bifurcation diagram corresponding to marginally stable nonuniform solutions. This asymptotic value of λ_c coincides with the value of λ at which an *infinite* pure A medium supports stationary, frontlike solutions. In a propagating bistable medium, self-similar front solutions $u(x,t) = u[x - c(\lambda)t]$ have the shape of kinks (heteroclinic orbits) connecting different steady states of the local kinetics. These fronts are stationary [$c(\lambda) = 0$] at the value $\lambda = \lambda_{\max}$ for which the Maxwell condition holds [6]:

$$\int_{u_-(\lambda)}^{u_+(\lambda)} F(u,\lambda,\alpha)\, du = 0\,,$$

where $u_-(\lambda)$ and $u_+(\lambda)$ are the extinguished and ignited steady states of the local kinetics. Frontlike solutions are translationally invariant in an infinite medium. The stationary solutions corresponding to the "vertical" branch in the bifurcation diagram of Fig. 2(a) appear as fragments of what would be stationary fronts in an infinite A medium at that parameter value; moving up the branch corresponds to the "translation" of the front fragment so that more and more of A becomes ignited [inset, Fig. 3(a)]. The intimate connection of these steady states with a self-similar "infinite-A" medium solution correlates with their practically neutral stability (leading eigenvalue of the linearization $\sim 10^{-4}$). A step change from $\lambda_1 < \lambda_{\max}$ to $\lambda_2 > \lambda_{\max}$ results in a *transient* ignition front which is initiated at the component interface and then invades domain A [Fig. 3(c)]. This analysis links the transient phenomenon of boundary-induced front initiation to infinite-medium nonuniform solutions, and associates the steady state branch close to the instability with stationary "translated" realizations of these fronts.

In extending our analysis to ignition from circular boundaries, we note that the solution profile in material B remains essentially flat over the whole domain for a wide range of λ values, while all spatial variation is confined to a *thin* boundary layer at the interface with medium A. We take advantage of this feature, and solve the two-domain problem in domain A *only*, with a boundary condition representing the effect of the "ignited B" neighbor. This Robin boundary condition, for A at the interface Σ with domain B, results through standard singular perturbation arguments after linearizing the corresponding partial differential equation (PDE) in B around a stable ignited branch u_+^B:

$$\left(\frac{\partial u}{\partial n} = \kappa\, \frac{u_+^B(\lambda,\alpha_B) - u}{\delta(\lambda)}\right)\Bigg|_\Sigma .$$

Here, $\delta(\lambda) = \sqrt{\frac{D}{\partial F(u,\lambda,\alpha_B)/\partial u}}$ is the "width" of the boundary layer in B, and the coefficient κ depends on the sign of the curvature of Σ [$K(I)_{0,1}$ are modified Bessel functions]:

$$\kappa = 1, \qquad \text{flat interface,}$$

$$\kappa = \frac{I_1[R/\delta(\lambda)]}{I_0(R/\delta(\lambda))} < 1, \qquad \text{concave interface,}$$

$$\kappa = \frac{K_1[R/\delta(\lambda)]}{K_0[R/\delta(\lambda)]} > 1, \qquad \text{convex interface.}$$

The accuracy of this boundary condition was tested by using it to reproduce the bifurcation results of the full, two-domain problem. It was then used to analyze the form of the nonuniform (partially ignited) branch for a circular domain A of radius R_A surrounded by a "sea" of material B.

The fact that κ differs from unity for curved interfaces has important consequences. The approximate translational invariance that led to the almost vertical branch of the bifurcation diagram for "striped" composites is lost in the case of circular inclusions. The curvature of the (in this case, concave) front increases as it moves away from the boundary, invading the circle. The speed of a radially symmetric (concave) front in a bistable system depends on curvature $c(\lambda, r) \approx c_{\text{flat}}(\lambda) + D/r$, where c_{flat} is the velocity of a flat interface asymptotically at small curvature;

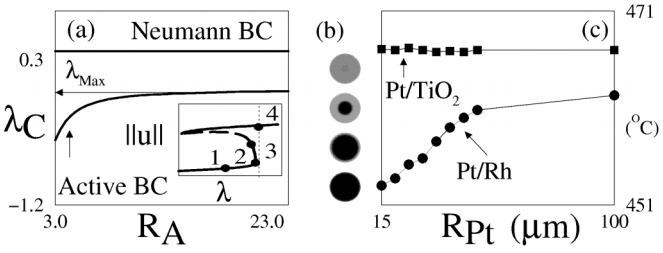

FIG. 4. Ignition of a circular inclusion: (a) Two-parameter diagram of turning points for domains with no-flux and active boundary conditions. (b) Sequence of steady states connecting extinguished and ignited states. (c) NO/CO reaction: Ignition temperatures of Pt circles surrounded by inert or active boundaries.

we then expect that the ignition of a circular domain will occur at a value below $\lambda_{\max}$. The analysis predicts that unstable (saddle-type) steady states existing past the turning point would appear as stationary fronts translated inwards; their progressively increasing curvature is compensated by the decrease in λ. Both predictions are confirmed by the continuation results shown in Figs. 4(a) and 4(b).

We have used the phenomenological model to explore the qualitative trends of ignition points for circular domains with inert or active boundaries. Data in Fig. 4(c), presenting the bifurcation properties of circular Pt domains, constitute an experimental confirmation of these trends. In these experiments the ignition temperature (T_{ign}) (at partial pressures $P_{\text{NO}} = 1.2 \times 10^{-5}$ mbar and $P_{\text{CO}} = 0.9 \times 10^{-5}$ mbar), corresponding to the transition from the unreactive to the reactive branch of the kinetic hysteresis, was measured as a function of the radius (R_{Pt}) of Pt circles. While T_{ign} is essentially constant for domains surrounded by inert TiO_2, it becomes an increasing function of R_{Pt} when the Pt circle is surrounded by more active Rh. This dependence saturates, as was predicted by the model, at large inclusion sizes. The process of (isothermal) ignition is initiated at the boundary of the circle and *propagates inwards*. The observations can be interpreted chemically as an effective *inflow* of empty sites into the Pt domain through its boundary with the more active Rh.

On the nanoscale, ignition initiated at crystal plane boundaries has been experimentally observed and addressed through Monte Carlo simulations [7]. For microcomposite catalysts, the thousandfold difference in length scales allowed us to use a continuum approach in linking this phenomenon to the bifurcation behavior of reaction-diffusion PDEs with active boundaries. Spatially nonuniform states caused by active boundary conditions have been previously reported for boundary fed reactors [8]. Our scalar caricature captures the essence of the behavior predicted by a (nongradient) multispecies mechanistic model [9]. This type of modeling will become increasingly predictive as its results are validated against measurements by other spatially resolving techniques. In particular, the nitrogen front accompanying (during ignition) the oxygen front [Fig. 2(d)] has been recently measured using scanning XPS [10]. We are currently exploring, both experimentally and computationally, the material design optimization problem of constructing a microcomposite surface with improved selectivity in NO reduction. The combination of controlled lithographic design with imaging and modeling opens, we believe, new avenues in exploring and understanding the dynamic operation of man-made and natural microreacting systems.

This work was partially supported by the National Science Foundation and the Alexander von Humboldt Foundation.

*Corresponding author.

[1] M. Sheintuch, J. Phys. Chem. **100**, 15 137 (1996); A. Hagberg, E. Meron, I. Rubinstein, and B. Zaltzman, Phys. Rev. Lett. **76**, 427 (1996); M. Bär, A. K. Bangia, I. G. Kevrekidis, G. Haas, H. H. Rotermund, and G. Ertl, J. Phys. Chem. **100**, 19 106 (1996).

[2] E. Schutz, N. Hartmann, I. G. Kevrekidis, and R. Imbihl, Catal. Lett. **54**, 181 (1998); J. Lauterbach, K. Asakura, P. B. Rasmussen, H. H. Rotermund, M. Bär, M. D. Graham, I. G. Kevrekidis, and G. Ertl, Physica (Amsterdam) **123D**, 493 (1998).

[3] M. D. Graham, I. G. Kevrekidis, K. Asakura, J. Lauterbach, K. Krischer, H. H. Rotermund, and G. Ertl, Science **264**, 5155 (1994); G. Haas, M. Bär, I. G. Kevrekidis, P. B. Rasmussen, H. H. Rotermund, and G. Ertl, Phys. Rev. Lett. **75**, 3560 (1995); N. Hartmann, M. Bär, I. G. Kevrekidis, K. Krischer, and R. Imbihl, Phys. Rev. Lett. **76**, 1384 (1996).

[4] A. G. Makeev and B. E. Nieuwenhuys, J. Chem. Phys. **108**, 3740 (1998); A. G. Makeev, M. M. Slinko, N. M. H. Janssen, P. D. Cobden, and B. E. Nieuwenhuys, J. Chem. Phys. **105**, 7210 (1996); R. Imbihl, T. Fink, and K. Krischer, J. Chem. Phys. **96**, 6236 (1992).

[5] M. Gruyters, A. T. Pasteur, and D. A. King, J. Chem. Soc. Faraday Trans. **16**, 2941 (1996); M. Tammaro and J. W. Evans, J. Chem. Phys **108**, 7795 (1998); H. Hirano, T. Yamada, K. I. Tanaka, J. Siera, P. Cobden, and B. E. Nieuwenhuys, Surf. Sci. **262**, 97 (1992).

[6] A. S. Mikhailov, *Foundations of Synergetics I* (Springer, Heidelberg, 1994), 2nd ed.

[7] V. Gorodetskii, J. Lauterbach, H. H. Rotermund, J. H. Block, and G. Ertl, Nature (London) **370**, 276 (1994); V. P. Zhdanov and B. Kasemo, Surf. Sci. **405**, 27 (1998).

[8] Q. Ouyang, V. Castets, P. DeKepper, and H. L. Swinney, J. Chem. Phys. **95**, 351 (1991); M. Bachir, P. Borckmans, and G. Dewel, Phys. Rev. E **59**, R6223 (1999).

[9] S. Y. Shvartsman, R. Imbihl, E. Schütz, and I. G. Kevrekidis (to be published).

[10] F. Esch, S. Gunther, E. Schuetz, A. Schaak, I. G. Kevrekidis, M. Marsi, M. Kiskinova, and R. Imbihl, Catal. Lett. **52**, 85 (1998).